MOLECULAR AND CELLULAR BIOLOGY, Apr. 2003, p. 2600–2607 Vol. 23, No. 7
0270-7306/03/$08.00+0 DOI: 10.1128/MCB.23.7.2600–2607.2003

Native Polycystin 2 Functions as a Plasma Membrane Ca^{2+}-Permeable Cation Channel in Renal Epithelia

Ying Luo,[1] Peter M. Vassilev,[2] Xiaogang Li,[1] Yoshifumi Kawanabe,[1] and Jing Zhou[1]*

Renal Division[1] and Endocrinology-Diabetes-Hypertension Division,[2] Department of Medicine, Brigham and Women's Hospital and Harvard Medical School, Boston, Massachusetts 02115

Received 28 October 2002/Returned for modification 11 December 2002/Accepted 8 January 2003

Mutations in polycystin 2 (PC2), a Ca^{2+}-permeable cation channel, cause autosomal dominant polycystic kidney disease. Whether PC2 functions in the endoplasmic reticulum (ER) or in the plasma membrane has been controversial. Here we generated and characterized a polyclonal antibody against PC2, determined the subcellular localization of both endogenous and transfected PC2 by immunohistochemistry and biotinylation of cell surface proteins, and assessed PC2 channel properties with electrophysiology. Endogenous PC2 was found in the plasma membrane and the primary cilium of mouse inner medullar collecting duct (IMCD) cells and Madin-Darby canine kidney (MDCK) cells, whereas heterologously expressed PC2 showed a predominant ER localization. Patch-clamping of IMCD cells expressing endogenous or heterologous PC2 confirmed the presence of the channel on the plasma membrane. Treatment with chaperone-like factors facilitated the translocation of the PC2 channel to the plasma membrane from intracellular pools. The unitary conductances, channel kinetics, and other characteristics of both endogenously and heterologously expressed PC2 were similar to those described in our previous study in *Xenopus laevis* oocytes. These results show that PC2 functions as a plasma membrane channel in renal epithelia and suggest that PC2 contributes to Ca^{2+} entry and transport of other cations in defined nephron segments in vivo.

Polycystins represent an expanding family of membrane proteins composed of two subfamilies, polycystin 1-like and polycystin 2-like molecules. PC1-like molecules consist of polycystin 1 (PC1) (1, 16), polycystin-REJ (15), polycystin-1L1 (40), and polycystin-1L2 (unpublished data), which likely function as unorthodox G protein-coupled receptors (5, 24). PC2-like molecules are ion channels and encompass PC2 (20), polycystin-L (4, 23, 38), and polycystin-2L2 (11). While the disease associations of the other polycystins are unknown, mutations in PC1 and PC2 cause autosomal dominant polycystic kidney disease, the leading genetic cause of renal failure. Formation of a large number of fluid-filled cysts in the kidney is the main characteristic of the disease.

PC1, encoded by *PKD1*, is predicted to be a ≈460-kDa integral membrane glycoprotein with a very large extracellular amino terminus, 11 transmembrane domains, and a small intracellular carboxyl terminus (1, 16). PC1 is found in the plasma membrane or in the cell-cell junction of cultured cells and in tissues (8, 17, 27). PC1 has recently been shown to function as a G protein-coupled receptor (5), although its ligand(s) has not been identified.

PC2, the product of *PKD2*, is predicted to encode an integral membrane protein of ≈110 kDa with an EF-hand domain at its carboxyl terminus (20). Sequence homology to other ion channels suggests a pore-forming capacity of PC2. Since mutations in PC1 and PC2 result in similar phenotypes and PC2 is able to interact with PC1 through its coiled-coil domain in vitro (28, 34), it has been speculated that PC1 and PC2 form a functional complex. However, data on the subcellular localization of PC2 have been controversial, in that both endoplasmic reticulum (ER) and plasma membrane localization have been reported. Immunostaining of PC2-transfected cells revealed an ER localization for PC2 (3). Membrane fractionation revealed that endogenous PC2 was mostly endoglycosidase H sensitive and was located in the ER fraction of kidney cells derived from mice overexpressing *PKD1* (22). In immunohistochemical investigations on tissue sections, PC2 was found in the basolateral membranes of renal tubules (7).

Besides these immunolocalization studies, our previous functional analyses revealed the presence of the same type of PC2 channel activity on both the intracellular and plasma membranes of *Xenopus laevis* oocytes that heterologously express PC2 (36). The property of PC2 as an intracellular calcium release channel has recently been confirmed by another study with the lipid bilayer method for reconstitution of channel activities in ER microsomes (19). However, patch-clamp experiments of Sf9 insect cells heterologously infected with PC2 detected PC2 on the plasma membrane (10). The functional site of the native PC2 channel in renal epithelia remains unknown.

In the present study, with a newly raised, highly specific antibody, we show that endogenous PC2 is localized in the plasma membrane and in the primary cilia of mouse inner medullar collecting duct (IMCD) cells and Madin-Darby canine kidney (MDCK) cells. Biotinylation of cell surface proteins confirmed the immunostaining data and revealed an increase of PC2 proteins in the plasma membrane of IMCD and MDCK cells overexpressing PC2. Results from patch-clamp studies on IMCD cells corroborated the biotinylation data. We provide evidence that the plasma membrane is a functional site for PC2 channel in renal epithelia.

* Corresponding author. Mailing address: Harvard Institutes of Medicine, Room 522, Brigham and Women's Hospital and Harvard Medical School, 4 Blackfan Circle, Boston, MA 02115. Phone: (617) 525-5860. Fax: (617) 525-5861. E-mail: zhou@rics.bwh.harvard.edu.

MATERIALS AND METHODS

DNA constructs. Full-length mouse *Pkd2* cDNA was cloned into pcDNA4/TO/Myc-His mammalian expression vector (Invitrogen), which utilizes a tetracycline-regulated expression system (T-Rex system; Invitrogen). With the removal of the stop codon in *Pkd2* cDNA, both Myc and histidine (His) epitope tags were added to the C terminus of PC2. Green fluorescent protein-tagged construct (Pkd2-GFP-pcDNA4) was generated by the insertion of the *hrGFP* cassette from vector phrGFP-1 (Stratagene) to the 3′ end of *Pkd2* in Pkd2-pcDNA4. The reading frame of both constructs was confirmed by DNA sequencing. ER-targeted yellow fluorescent protein (YFP) construct pEYFP-ER (Clontech) was used as an ER marker for transiently transfected cells.

Cell culture and transient and stable transfections. IMCD (ATCC catalog no. CRL-2123) and MDCK cells were cultured in Dulbecco's modified Eagle's medium/F12 medium supplemented with 10% (vol/vol) fetal bovine serum (Invitrogen). LLC-PK1, HEK293T, and 293T-S-PC2 (stably expressing PC2) cell lines were cultured in Dulbecco's modified Eagle's medium with 10% (vol/vol) fetal bovine serum. In 293T-S-PC2 cell culture, zeocin (200 μg/ml) and blasticidin (5 μg/ml) (Invitrogen) were added. For induction, 1 μg of tetracycline per ml was added to the medium.

Transient transfections were carried out on cells cultured to 30% to 50% confluency. DNA constructs were transfected with Fugene 6 transfection reagent (Roche) following the protocol from the manufacturer. Forty-eight hours after the transfection, cells were harvested for further analysis.

For stable transfection, Pkd2-pcDNA4 vector was transfected with Fugene 6 transfection reagent (Roche) into commercially available HEK293T cells that were stably transfected with a tetracycline regulator vector, pcDNA/TR (Invitrogen). After 48 h, the antibiotics zeocin (200 μg/ml) and blasticidin (5 μg/ml) were added to the selective culture medium. After 1 month, single isolated colonies were picked and screened for the expression of PC2 by immunofluorescence. Positive clones were amplified and confirmed by immunoprecipitation before and after induction with tetracycline.

Antibodies. Anti-PC2 polyclonal antibody 96525 was raised in rabbits against a peptide (EQRGLEIEMERIRQAAARD) in the N-terminal intracellular domain of PC2 (amino acids 44 to 62 in the mouse, corresponding to amino acids 48 to 66 with an E to Q substitution in humans). The antibody was purified with an affinity column with the immunizing peptide according to standard procedure (Research Genetics). Purified antibody was used at a 1:500 dilution for immunofluorescence, 1:50 for immunoprecipitation, and 1:1,000 for Western blotting.

Mouse monoclonal antibodies against E-cadherin or p120 (BD Biotransduction Laboratories) were used as a membrane marker for immunofluorescence at 1:200 dilution. Mouse monoclonal antibody against the Myc tag (Invitrogen) was used at 1:500 for immunoprecipitation and for immunofluorescence. Mouse monoclonal antibody against the His tag (Santa Cruz) was used at 1:5,000 for Western blotting. Polyclonal antibody against calnexin (Stressgen) was used at 1:5,000 for Western blotting and 1:200 for immunofluorescence.

Goat anti-rabbit immunoglobulin G (IgG)-fluorescein isothiocyanate (FITC) and goat anti-mouse IgG-Texas Red (Vector) were used as secondary antibodies for immunofluorescence at a dilution of 1:500. For Western blotting, goat anti-rabbit IgG-horseradish peroxidase and goat anti-mouse IgG-horseradish peroxidase, 1:10,000 dilution (Amersham Pharmacia Biotech), were used as secondary antibodies.

Immunoprecipitation and Western blotting. Immunoprecipitation was performed as described by the manufacturer (Upstate Biotechnology Inc.). Proteins were then electrotransferred to enhanced chemiluminescence (ECL) nitrocellulose membranes (Amersham Pharmacia Biotech). For Western blotting, blots were preincubated with blocking buffer (10% dry milk, 0.1% Tween 20 in 1× phosphate-buffered saline [PBS]) for at least 1 h, followed by incubation with primary and secondary antibodies in blotting buffer (1% dry milk, 0.1% Tween 20 in 1× PBS), and detection with the ECL system (Amersham Pharmacia Biotech). For peptide blocking, antibody was preincubated with specific peptide at 4°C overnight. The preabsorbed antibody was used for Western blotting as described above.

Immunofluorescence. Immunofluorescence technique was modified from a previously published method (13). Briefly, cells were fixed with 3% paraformaldehyde and 2% sucrose in 1× PBS (pH 7.6) for 10 min, followed by 5 min of treatment with 1% NP-40 in 1× PBS to permeabilize membranes. After preincubation with 5% bovine serum albumin–PBS, cells were incubated with specific primary antibody in 1% bovine serum albumin–PBS for 1 h at room temperature. After washing, secondary antibodies were incubated for 1 h. Prolong mounting medium (Molecular Probes) was used to protect immunofluorescence signals from fading. Zeiss Axioskop2 Plus fluorescence microscope (Carl Zeiss, Inc.) was used to observe the signal, and the Spot camera system (Diagnostic Instruments, Inc.) was used to take pictures. Confocal microscope 1024 MRC (Kr/Ar laser) (Bio-Rad) was used to acquire images of cilia without background from cell membranes. To show some length of the cilia, images from five consecutive optical sections were combined.

Biotinylation of cell surface proteins. IMCD and MDCK cells at ≈30% confluence were transfected with or without the Pkd2-pcDNA4 construct. Forty-eight hours after transfection, cell surface proteins were labeled with 15-([biotinoyl]amino)-4,7,10,13-tetraoxapentadecanoic acid–*N*-hydroxysuccimidyl ester (NHS-PEO_4-biotin; Pierce) following the instruction provided by the manufacturer. Briefly, cells were washed with 1× PBS (pH 7.2) three times, and then NHS-PEO_4-biotin (0.5 mg/ml) was added and incubated at room temperature for 30 min. After washing cells with 1× PBS three times, radioimmunoprecipitation assay (RIPA) buffer was added to lyse the cells. After preclearing the lysates with protein A-agarose beads (Pierce), biotinylated proteins were further pulled down by monomeric avidin beads and eluted by 2 mM free D-biotin (Pierce). Eluted samples were mixed with 3× SDS loading buffer, boiled for 5 min, and loaded on a sodium dodecyl sulfate–7.5% polyacrylamide gel for electrophoresis.

Electrophysiological techniques. Patch-clamp techniques for obtaining cell-attached or excised membrane patches were used as described (12). The pipette solution contained, unless otherwise specified, 100 mM KCl, 0.1 mM $CaCl_2$, and 10 mM HEPES, pH 7.5. In some experiments, 100 mM KCl was substituted with 100 mM NaCl or equal amounts of other salts as described in the figure legends. When filled with this external solution, the pipette tip resistances were 5 to 10 MΩ. Seals with resistances of >5 GΩ were employed in single channel experiments, and currents were measured with an integrating patch-clamp amplifier. Single channel currents were filtered at 3 to 10 kHz through an 8-pole Bessel filter. The bath solution contained, unless otherwise specified, 100 mM KCl, 0.1 μM $CaCl_2$, 10 mM HEPES, and 5 mM EGTA, pH 7.5. The concentrations of Ca^{2+} in solutions containing low Ca^{2+} (0.1 to 1 μM) were adjusted according to a previous study (32).

Analysis of electrophysiological data. Voltage stimuli were applied and single channel currents were digitized (50 to 150 μs per point) and analyzed with a PC, a Digidata converter, and programs based on pClamp (Axon Instruments). Open state probability (Po) was calculated from 30- to 50-s segments of current records in patches containing apparently only one functioning channel, since only one current level was observed in these recordings. Several hundred or more events were analyzed with half-amplitude threshold criteria for generating each data point. The Goldman-Hodgkin-Katz (GHK) equation was used to calculate the permeability ratios between a defined cation (P_X) and K^+ (P_K): $E_{rev} = RT/F \ln [P_X/P_K]$, where E_{rev} is the change in reversal potential measured when K^+ is replaced by Na^+ or other cations in the pipette solution, R is the gas constant, T is the absolute temperature, and F is Faraday's constant. The experiments were carried out at 23°C. Four or more experiments were performed for each condition to determine statistical differences.

Measurements of intracellular Ca^{2+}. Coverslips with cells were loaded for 1 h at 37°C under reduced light with fura-2/acetoxymethyl ester (10 μM) in Krebs-HEPES buffer (140 mM NaCl, 3 mM KCl, 1 mM $MgCl_2$, 11 mM glucose, 10 mM HEPES, pH 7.3). The coverslips were then placed diagonally in a thermostatted quartz cuvette containing Krebs-HEPES buffer and used for measuring fluorescence with a Delta Scan-1 microfluorometer (Photon Technology International). Excitation monochrometers were centered at 340 and 380 nm, and emission light was collected at 510 nm. At the end of the experiment, Triton X-100 and then EGTA were added to final concentrations of 0.1% and 5 mM, respectively, in order to measure the fluorescence maximum (F_{max}) and minimum (F_{min}). The internal Ca^{2+} concentration ($[Ca^{2+}]_i$) was determined from the ratio of fura-2 fluorescence at 340 nm to that at 380 nm according to the manufacturer's instructions (Molecular Probes).

RESULTS

Generation and characterization of an anti-PC2 antibody (96525). An anti-PC2 antibody (96525) was raised in rabbits to a peptide in the N-terminal cytoplasmic domain of mouse PC2 (residues 44 to 62). This sequence is highly conserved among the mouse, canine, and human PC2 proteins. Both anti-His and anti-PC2 (96525) antibodies recognized a strong ≈110-kDa band immunoprecipitated by an anti-Myc antibody in cells transiently transfected with full-length PC2 but not in untransfected cells (Fig. 1A). The PC2 band recognized by 96525

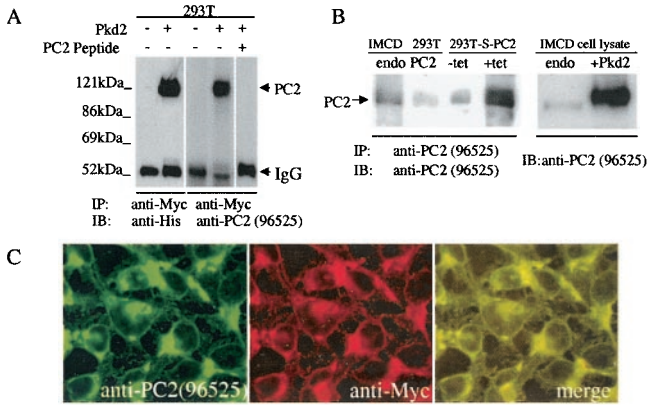

FIG. 1. Characterization of anti-PC2 antibody 96525. (A) Characterization of 96525 by Western analyses. 293T cells with or without transient transfection of Pkd2-pcDNA4 were immunoprecipitated with an anti-Myc tag antibody, followed by immunoblotting with either an anti-His tag antibody or 96525. A strong ≈110-kDa band was recognized by both antibodies. Preincubation with a PC2-specific peptide completely blocked the signal. (B) Characterization of 96525 by immunoprecipitation and Western blotting. Left panel, endogenous PC2 in IMCD and 293T cells, as well as overexpressed PC2 from the inducible stable cell line 293T-S-PC2, was immunoprecipitated by 96525, followed by immunoblotting with the same antibody. Stronger endogenous PC2 expression can be seen in IMCD cells than in 293T cells. PC2 expression in the PC2 stably transfected cell line greatly increased upon tetracycline induction. Right panel, Western analysis of IMCD cells with or without transient transfection of PC2. Antibody 96525 recognized both endogenous and transiently transfected PC2. (C) Double labeling with 96525 and anti-Myc tag antibodies revealed a completely overlapping localization pattern for PC2 in 293T-S-PC2 cells with induced PC2 expression.

could be blocked by preincubation of this antibody with its immunogen (Fig. 1A), demonstrating that antibody 96525 recognized PC2 specifically.

Antibody 96525 was able to immunoprecipitate endogenous PC2 in several different cell lines, including IMCD and HEK293T (Fig. 1B). It also recognizes both endogenous and transient transfected PC2 by Western blot (Fig. 1B), and no cross-reactive bands were detected. To further characterize this antibody, we established a HEK293T cell line that stably expresses PC2 (293T-S-PC2) in a tetracycline-inducible system and used 96525 to immunoprecipitate and immunoblot PC2 in 293T-S-PC2 cells before and after induction of PC2 expression. We detected very strong expression of PC2 after induction, as expected (Fig. 1B), although a higher level of PC2 expression was detected in uninduced 293T-S-PC2 cells than in untransfected cells, which was likely due to a leakage of the inducible system (Fig. 1B). Double labeling with 96525 and an anti-Myc tag antibody revealed a completely overlapping localization pattern for PC2 in 293T-S-PC2 cells with induced PC2 expression (Fig. 1C), demonstrating the specificity of 96525 in immunostaining.

Subcellular localization of endogenous PC2 in IMCD and MDCK cells. We observed distinct plasma membrane labeling of PC2 in IMCD and MDCK cells with 96525 (Fig. 2A and J). Double labeling of PC2 with a plasma membrane-associated protein, p120 (Fig. 2B), and a plasma membrane protein E-cadherin (Fig. 2K) indicated a plasma membrane location for PC2. PC2 was also found in the primary cilia of IMCD (Fig. 2D) and MDCK (Fig. 2M) cells, as demonstrated by colocalization with a ciliary marker, acetylated α-tubulin (Fig. 2E, F, N, and O), which is consistent with a recent report (26). PC2 labeling on both membrane and cilia was blocked by preincu-

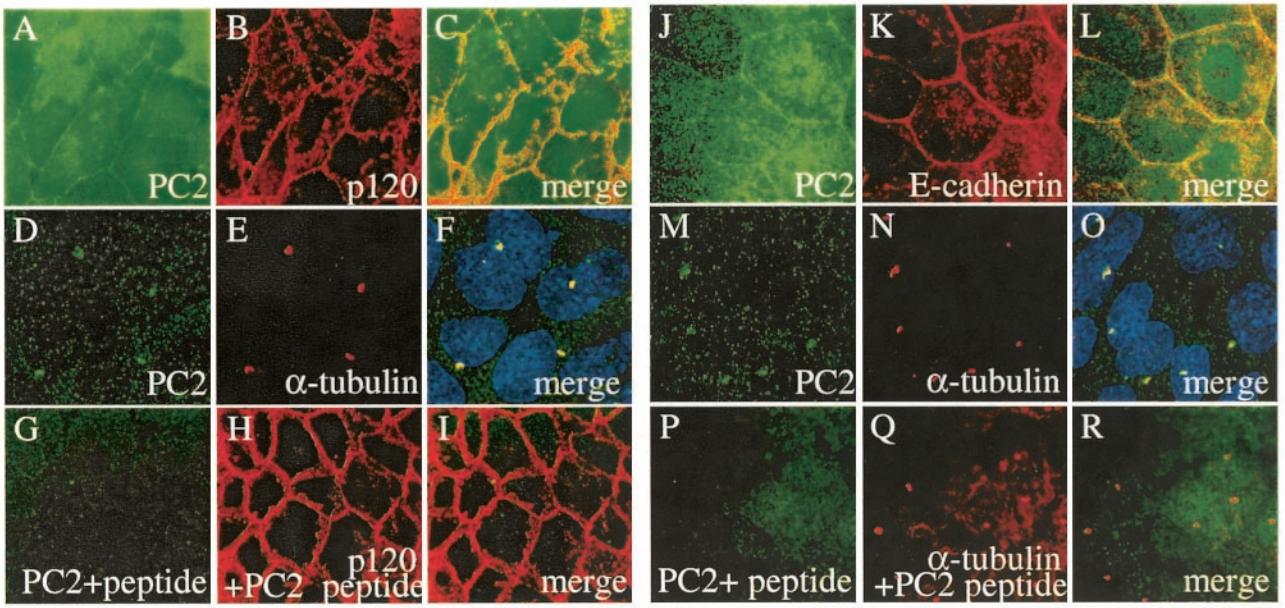

FIG. 2. Plasma membrane and cilia localization of PC2 in IMCD and MDCK cells. Double labeling of IMCD (A to C) or MDCK (J to L) cells by the anti-PC2 antibody 96525 (A, J) and anti-p120, a cell plasma membrane-associated protein (B), or anti-E-cadherin, a plasma membrane protein (K), localizes PC2 to cell plasma membrane (C, L). Double labeling of IMCD (D to F) or MDCK (M to O) cells by 96525 (D, M) and a cilia marker, acetylated α-tubulin (E, N), showed that PC2 is also localized to the monocilia in these cells. Preincubation with a PC2-specific peptide completely blocked the PC2 signal (G, P) but not the membrane or cilia marker (H, I, Q, R).

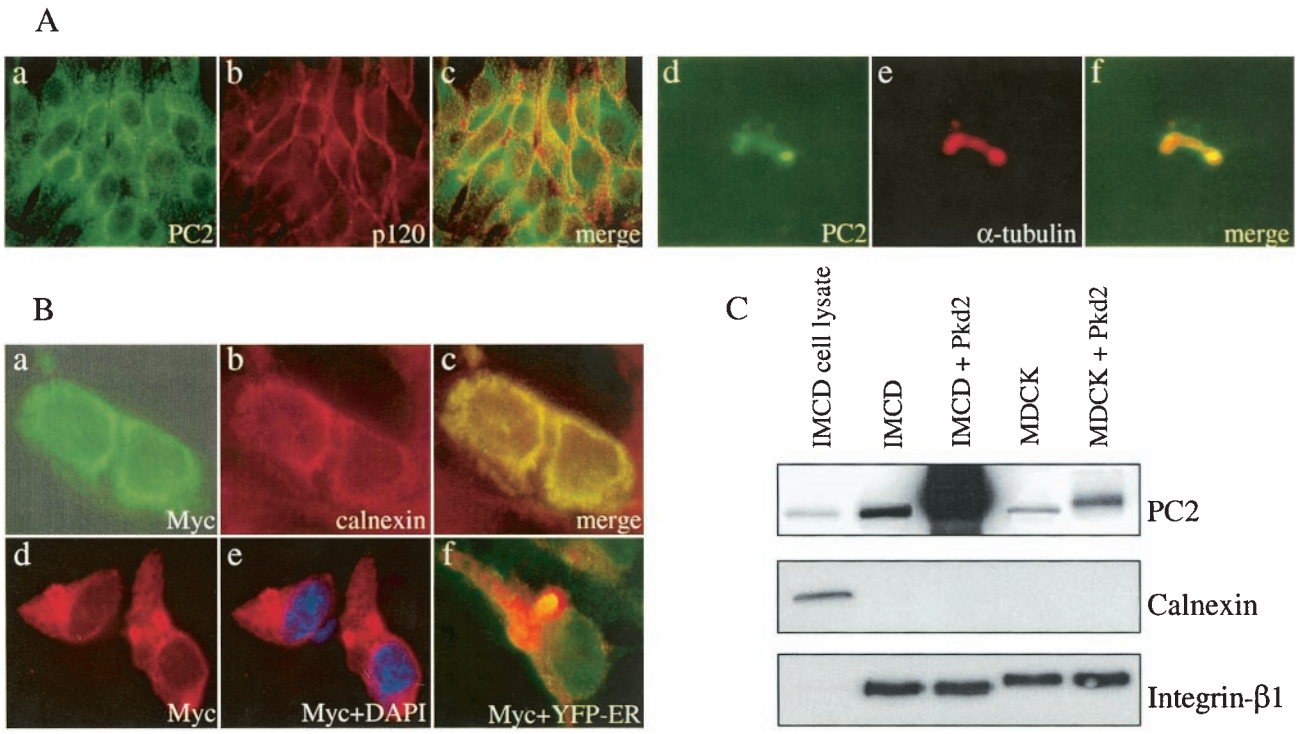

FIG. 3. Endogenous and heterologously expressed PC2 localization. (A) Endogenous PC2 localization in LLC-PK1 cells. Endogenous PC2 is primarily seen in the cytoplasm (a to c) and cilia (d to f) of LLC-PK1 cells with the PC2 antibody 96525. PC2 does not colocalize with the plasma membrane marker p120 (b, c). (B) Subcellular localization of heterologously expressed PC2. Double labeling of IMCD cells transfected with full-length *Pkd2* with an anti-Myc antibody (B, a) and an anti-ER marker (calnexin) antibody (B, b) revealed that PC2 colocalizes with calnexin in the ER (B, c). Double labeling of 293T-S-PC2 cells with an anti-Myc antibody (B, d) and the nuclear marker 4′,6′-diamidino-2-phenylindole (DAPI) (B, e) shows PC2 in the nuclear membrane. Transiently transfected 293T-S-PC2 cells with the ER marker YFP-ER revealed an ER localization of stably overexpressed PC2 (B, f). (C) Biotinylation of cell surface proteins of IMCD or MDCK cells with or without transient transfection of Pkd2-pcDNA4. Increased PC2 proteins on cell membranes were observed by immunoblotting with 96525 (top). An ER marker, calnexin, was used as a negative control (middle), and a cell membrane marker, β1-integrin, was used as a positive control (bottom).

bation of the antibody with the PC2 peptide used to raise the antibody (Fig. 2G and P), while the signals for p120 (Fig. 2H and I) or acetylated α-tubulin (Fig. 2Q and R) remained. These data demonstrate the specificity of the plasma membrane and cilia patterns of PC2 in immunostaining. Interestingly, with the same antibody, we found endogenous PC2 in the cytoplasm of LLC-PK1 cells (Fig. 3A, a). We did not detect PC2 colocalization with the membrane marker p120 (Fig. 3A, b and c), although we did detect PC2 in the cilia (Fig. 3A, d to f). Subcellular localization of endogenous PC2 in HEK293T cells was also studied and revealed a strong cytoplasmic and a weak plasma membrane staining pattern (data not shown).

Subcellular localization of heterologously expressed PC2 in IMCD cells by immunostaining. To investigate whether overexpression of PC2 alters its subcellular localization in IMCD cells, we transiently transfected these cells with a full-length *Pkd2* construct, Pkd2-pcDNA4. Double labeling of PC2 with anti-Myc antibody (Fig. 3B, a) and an ER marker, calnexin (Fig. 3B, b), revealed an ER localization of overexpressed PC2 proteins (Fig. 3B, c). However, due to the continuous signals between the cytoplasm and cell plasma membrane, it was difficult to determine, under the resolution of the light microscope, whether a small fraction of heterologously expressed PC2 was targeted to the cell plasma membrane. In 293T-S-PC2 cells, stably overexpressed PC2 colocalized with an ER marker, YFP-ER (Fig. 3B, f). We also noticed some labeling in nuclear membrane staining (Fig. 3B, d and e).

Plasma membrane localization of PC2 revealed by biotinylation of cell surface proteins. To further study the plasma membrane localization of PC2 revealed by immunostaining, we biotinylated cell surface proteins in IMCD and MDCK cells with and without heterologously expressed PC2. Notably, biotinylated endogenous PC2 was found in IMCD and MDCK cells, suggesting a plasma membrane localization of endogenous PC2 in these cells (Fig. 3C, top). Interestingly, overexpression of PC2 dramatically increased the amount of biotinylated PC2 in both cell types (Fig. 3C, top). The biotinylated membrane fraction does not appear to contain a detectable amount of ER membranes since we did not detect calnexin, an ER protein marker (Fig. 3C, middle). The enrichment of cell membrane proteins in the biotinylated fraction was confirmed with integrin β1 as a membrane marker (Fig. 3C, bottom).

PC2 channel activity in IMCD cells. To test whether the PC2 proteins are functional in these cells and display channel properties similar to those in other cell types that we characterized previously (36), we carried out electrophysiological studies with the patch-clamp technique. In cell attached patches with 100 mM KCl or 100 mM NaCl in the pipette solution, we frequently observed channel activities (46 of 118 patches) with characteristic bursts of brief openings and clos-

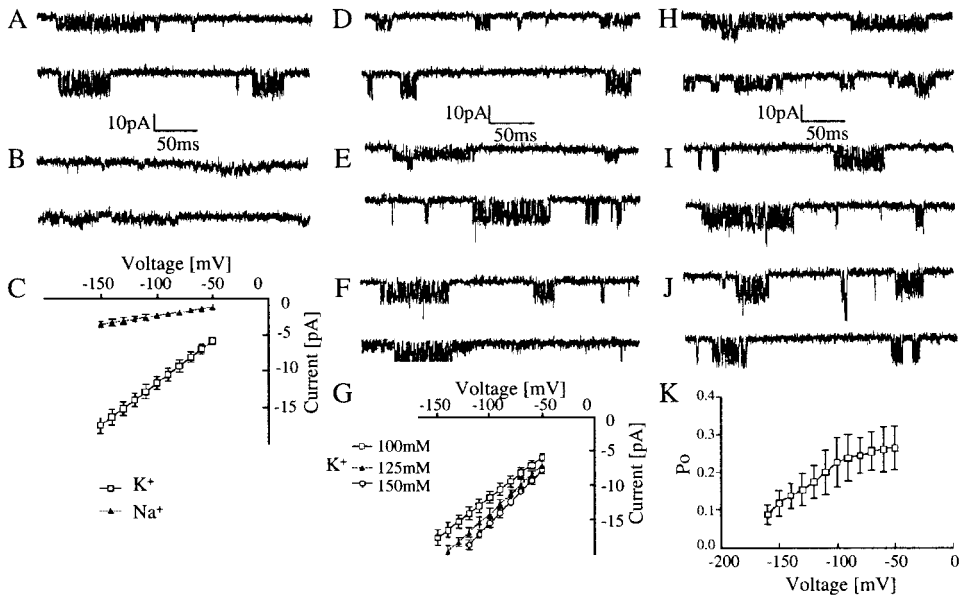

FIG. 4. Characteristics of endogenous PC2 channels in IMCD cells. (A to C) Single PC2 channel activities in IMCD cells in the presence of 100 mM K^+ (A) or Na^+ (B) in the external pipette solution. The tracings were taken at −70 mV (top traces) and −130 mV (bottom traces). Current-voltage relations determined in the presence of K^+ (open squares) or Na^+ (solid triangles) are shown in panel C. (D to G) Comparison between the channel activities recorded in the presence of various K^+ concentrations in the pipette solution: 100 mM (D), 125 mM (E), and 150 mM (F). Current-voltage relations determined in the presence of 100 mM K^+ (open squares), 125 mM K^+ (solid triangles), and 150 mM K^+ (open circles) are shown in G. (H to K) Dependence of the PC2 channel activities upon the applied voltage. Current traces were taken at −70 mV (H), −120 mV (I), and −150 mV (J). The probability of the open state (Po) as a function of voltage is plotted (K). Downward deflections represent negative inward currents.

ings (Fig. 4A and B). The difference between the conductances of the two cations is shown in Fig. 4C. The unitary conductances determined from the slopes of the current-voltage relations were 116.2 ± 13.5 pS (mean ± standard error of the mean, $n = 14$) for K^+ and 23.6 ± 4.2 pS ($n = 8$) for Na^+ in the presence of either of the cations at 100 mM. The permeability ratio, P_{Na}/P_K, was 0.19. The amplitudes of the channel openings increased with elevation in the K^+ concentration in the pipette solution (Fig. 4D to G). The single channel conductances determined from the slopes of the current-voltage relations were substantially larger at higher K^+ concentrations (Fig. 4G), showing that the channels are highly permeable to K^+ as we described previously in the study on PC2 channels functionally expressed in oocytes (36).

We also determined the conductances and permeabilities of the PC2 channels to other cations. The conductance in the presence of NH_4^+ as a charge carrier was 92.8 ± 7.4 pS ($n = 4$) in nontransfected IMCD cells and 93.2 ± 8.1 pS ($n = 6$) in PC2-transfected cells. The permeability ratios, P_{NH4}/P_K, were 0.71 for the endogenous PC2 and 0.73 for the heterologously expressed PC2, respectively. The conductance of Rb^+ was 67.1 ± 9.2 pS ($n = 4$) in nontransfected cells and 66.7 ± 7.8 pS ($n = 5$) in PC2-transfected cells. These values are almost identical to those of the PC2 channels measured in *Xenopus laevis* oocytes as described in our previous study (36). Channel activities characterized with more frequent opening and longer bursts in the presence of K^+ as a charge carrier were observed in IMCD cells transiently transfected with PC2 (Fig. 5D, E, and H).

Although we did not observe obvious voltage dependence for the PC2 channel in the physiological voltage range in these cells, as in oocytes (36), a characteristic voltage dependence of the Po was seen at more negative voltages (Fig. 4H to J). Po decreased substantially at voltages more negative than −100 mV (Fig. 4K). We varied the content of anions and cations in the solutions on both sides of the inside-out patches and found that Cl^- influx or efflux does not contribute substantially to the currents.

To determine the unitary conductance of the PC2 channels to Ca^{2+}, we were able to measure the current amplitudes only when with high concentrations of Ca^{2+} on the extracellular sides of the patches (Fig. 5A to C). The channel activity usually occurred in characteristic bursts of brief openings in both untransfected (Fig. 5A) and PC2-transfected (Fig. 5B) IMCD cells. The current-voltage relationship in the latter type of cells is slightly less linear than in the former one (Fig. 5C). The Ca^{2+} conductance, measured over the linear voltage range (−60 to −100 mV), however, was similar for both types of cells, 37.8 ± 3.26 pS ($n = 8$) for untransfected and 39.2 ± 4.35 pS ($n = 6$) for PC2-transfected cells. These values are slightly higher than that measured in oocytes, 36.4 pS (36). We also compared the conductance of Ca^{2+} with that of another divalent cation, Ba^{2+}. In the presence of this cation as a charge carrier, the conductance was 46.2 ± 3.7 pS ($n = 5$) in nontransfected IMCD cells and 46.7 ± 4.5 pS ($n = 7$) in PC2-transfected cells. Thus, the properties of both endogenous and heterologously expressed PC2 channels in IMCD cells described in the present study are the same as those characterized in our previous study on PC2 channels in *Xenopus laevis* oocytes (36).

To determine whether targeting of PC2 to the plasma mem-

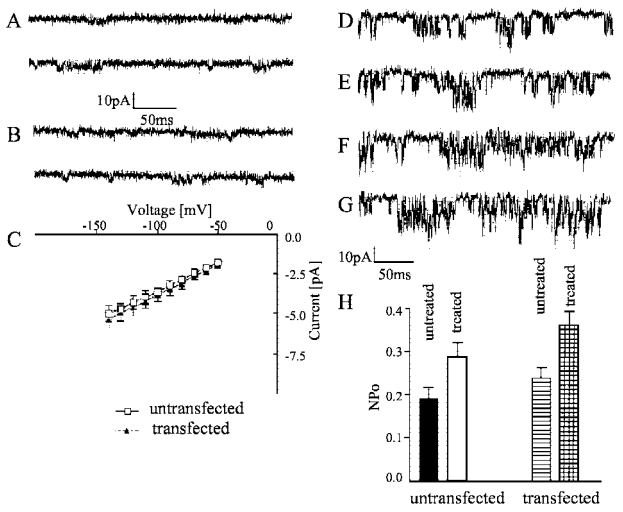

FIG. 5. PC2 overexpression and treatment with chaperone-like factors in IMCD cells result in an increased PC2 channel open probability. (A to C) Single Ca^{2+} channel currents in untransfected (A) and PC2-transfected (B) cells were taken at −70 mV (top traces) and −120 mV (bottom traces). The current-voltage relations for untransfected (open squares) and PC2-transfected (solid triangles) cells are shown (C). The current records were taken in cell-attached patches in the presence of 100 mM $CaCl_2$ in the pipette solution. (D to G) Comparison between the channel activities in untransfected (D, F) and PC2-transfected (E, G) cells. The PC2 channel activities were recorded at −120 mV in cell-attached patches of untreated cells (D, E) or cells that had been treated for 48 h with a combination of 5 μM lactacystin, 5 μM *N*-acetyl-Leu-Leu-norleucinal, and 10 mM trimethylamine-*n*-oxide (F, G). The NPo determined in patches of cells treated or not treated with these agents are compared (H). The values represent the mean ± standard error of the mean ($n = 6$).

brane in mammalian cells (36) can be facilitated by proteasome inhibitors and chemical chaperone-like factors (2, 6, 18, 29, 35, 37), we treated untransfected and PC2-transfected IMCD cells with such agents. The level of PC2 channel activity in the plasma membranes of both untransfected and PC2-transfected cells increased after treatment of the cells for 48 h (Fig. 5D to G). A more substantial increase in channel activity, however, was observed in PC2-transfected cells (Fig. 5F and G), as evidenced by measuring the open state probability multiplied by the number of channel current levels (NPo) (Fig. 5H). However, the magnitude of increase of the PC2 channel activity is not as great as that of the cell surface protein levels. This may partly be due to the need of multiple subunits to form a pore and the fact that the channels are at a resting status. There are no significant differences in the basal levels of intracellular Ca^{2+} concentration bwtween IMCD cells with or without overexpressed PC2 (32.5 ± 3.5 nM, mean ± standard error, $n = 6$, versus 31.7 ± 6.5 nM, mean ± standard error, $n = 6$).

DISCUSSION

The PC2 channels in IMCD cells are of striking similarity to those in oocytes as described earlier (36), but with slightly smaller conductances and less pronounced voltage dependence. Such differences have been described for other types of channels and may be attributed to the presence of different intracellular enzymes or other regulatory factors in mammalian cells versus *Xenopus* oocytes. There are many similarities but also some differences between our data and those described in artificial bilayers and other membranes (9, 19). They may be explained by the different approaches, experimental conditions and expression systems used in these studies. It has been established that the properties of many types of channels can vary significantly from one type of native or reconstituted model membrane to another depending on specific binding partners, phospholipid environment, fluidity, and other membrane biophysical characteristics.

PC2 protein has been found in the ER of LLC-PK1 cells (3) and Chinese hamster ovary (CHO) cells (13), in the plasma membrane of MDCK cells (30), and in the apical and basolateral plasma membranes in tubular structures in vivo (7). Knowledge of the site of PC2 action is critical for our understanding of PC2 function and the pathogenesis of autosomal dominant polycystic kidney disease. Here we show that endogenous PC2 is present on the plasma membranes of IMCD and MDCK cells but in the cytoplasm of LLC-PK1 cells with the PC2 antibody 96525. These data indicate that the localization of PC2 is cell type specific, clarifying the controversy on endogenous PC2 localization.

Interestingly, we found PC2 expression in the primary cilia of all three types of renal epithelia examined despite the differences in plasma membrane localization, which suggests a conserved role of PC2 in the primary cilia. A role of cilia in polycystic kidney disease has recently been suggested by the ciliary localization of polaris and cystin, proteins mutated in two *PKD* mouse models (14, 25, 31, 39). The expression of PC2 in the cilia of both IMCD and MDCK cells is consistent with a role of PC2 on the plasma membrane, where it possibly participates in the mechanosensory function of cilia (21) and mediates Ca^{2+} entry and Ca^{2+} signaling in renal epithelia.

Previous reports revealed that heterologously expressed PC2 proteins were predominately localized to the ER of MDCK cells (3, 30). Here, with immunofluorescence, we found predominant localization of overexpressed PC2 in the ER of IMCD cells; however, by biotinylation of cell surface proteins, we found a dramatic increase of PC2 in the plasma membrane of IMCD or MDCK cells transiently overexpressing PC2. This observation was further supported by patch-clamp studies, which revealed an increase of PC2 channel activity in IMCD cells transiently transfected with PC2. The effect was most pronounced after treatment of the cells with chaperone-like factors. Together, these data suggest that overexpression of PC2 in the cell types examined increases its translocation from the ER to the plasma membrane.

We previously showed that in oocytes, PC2 channel activity is predominantly present in the nuclear membranes that are continuous with ER membranes, with a low density of channels in the plasma membranes (36). The functionality of PC2 channel in the ER has recently been confirmed (19). In the latter study, however, the channel activities were reconstituted in lipid bilayer, an approach that does not allow direct in situ measurements of the channel currents in their native environment in the ER or plasma membranes. Based on our current data, together with recently reported immunolocalization of PC2 (30), the detection of PC2 chan-

nel activity in plasma membranes of syncytiotrophoblasts (9), and the finding of a small amount of PC2 in plasma membrane fraction of human kidneys (22), we propose that the plasma membrane can serve as one of the functional sites for the native PC2 channel. Consequently, we believe that PC2 is involved in Ca^{2+} entry in defined renal epithelial cells and other ionic fluxes across their plasma membranes with potential implications in Ca^{2+} reabsorption and related mineral ion homeostatic processes. The means by which PC2 is translocated to the membrane is currently unknown but could involve the assistance of PC1 (13) or an interaction with transient receptor potential channel (TRPC1) (33), or through other yet to be identified mechanisms. The limited increase of PC2 channel activity in plasma membrane of cells overexpressing PC2 suggests that the rate of its membrane targeting may be limited by endogenous protein targeting machinery.

It is known that under defined conditions, channels usually residing in the ER can be translocated to plasma membrane where they function. The epithelial Na^+ channel, for example, is predominantly located on ER membranes, but depending on defined turnover mechanisms and other factors, it mediates Na^+ reabsorption across the plasma membranes of renal cells. Similar to PC2, its translocation to the plasma membrane can be promoted by proteasome inhibitors and other agents that inhibit protein degradation (35). We do not exclude, however, a role of PC2 in the ER. Its function on plasma membrane and ER may be tightly regulated upon cell differentiation status and dynamics of the PC2 protein complex such as ligand binding to its interaction partner(s) (e.g., PC1), cell cytoskeletal rearrangements, or other stimuli. We believe that the controversies regarding the localization of PC2 are due to the differences between the specific cell types, the differentiation status of the cells, or the growth factors and ionic composition of the medium used in various studies.

ACKNOWLEDGMENTS

This work was supported by grants from the National Institutes of Health (NIDDK) to J.Z. and from the PKR Foundation to P.M.V.

The first two authors contributed equally to this work.

REFERENCES

1. **Anonymous.** 1995. Polycystic kidney disease: the complete structure of the PKD1 gene and its protein. The International Polycystic Kidney Disease Consortium. Cell **81:**289–298.
2. **Brown, C. R., L. Q. Hong-Brown, and W. J. Welch.** 1997. Correcting temperature-sensitive protein folding defects. J. Clin. Investig. **99:**1432–1444.
3. **Cai, Y., Y. Maeda, A. Cedzich, V. E. Torres, G. Wu, T. Hayashi, T. Mochizuki, J. H. Park, R. Witzgall, and S. Somlo.** 1999. Identification and characterization of polycystin-2, the PKD2 gene product. J. Biol. Chem. **274:** 28557–28565.
4. **Chen, X. Z., P. M. Vassilev, N. Basora, J. B. Peng, H. Nomura, Y. Segal, E. M. Brown, S. T. Reeders, M. A. Hediger, and J. Zhou.** 1999. Polycystin-L is a calcium-regulated cation channel permeable to calcium ions. Nature **401:**383–386.
5. **Delmas, P., H. Nomura, X. Li, M. Lakkis, Y. Luo, Y. Segal, J. M. Fernandez-Fernandez, P. Harris, A. M. Frischauf, D. A. Brown, and J. Zhou.** 2002. Constitutive activation of G-proteins by polycystin-1 is antagonized by polycystin-2. J. Biol. Chem. **277:**11276–11283.
6. **Denning, G. M., M. P. Anderson, J. F. Amara, J. Marshall, A. E. Smith, and M. J. Welsh.** 1992. Processing of mutant cystic fibrosis transmembrane conductance regulator is temperature-sensitive. Nature **358:**761–764.
7. **Foggensteiner, L., A. P. Bevan, R. Thomas, N. Coleman, C. Boulter, J. Bradley, O. Ibraghimov-Beskrovnaya, K. Klinger, and R. Sandford.** 2000. Cellular and subcellular distribution of polycystin-2, the protein product of the PKD2 gene. J. Am. Soc. Nephrol. **11:**814–827.
8. **Geng, L., Y. Segal, B. Peissel, N. Deng, Y. Pei, F. Carone, H. G. Rennke, A. M. Glucksmann-Kuis, M. C. Schneider, M. Ericsson, S. T. Reeders, and J. Zhou.** 1996. Identification and localization of polycystin, the PKD1 gene product. J. Clin. Investig. **98:**2674–2682.
9. **Gonzalez-Perret, S., K. Kim, C. Ibarra, A. E. Damiano, E. Zotta, M. Batelli, P. C. Harris, I. L. Reisin, M. A. Arnaout, and H. F. Cantiello.** 2001. Polycystin-2, the protein mutated in autosomal dominant polycystic kidney disease (autosomal dominant polycystic kidney disease), is a Ca^{2+}-permeable nonselective cation channel. Proc. Natl. Acad. Sci. USA **98:**1182–1187.
10. **Gonzalez-Perrett, S., M. Batelli, K. Kim, M. Essafi, G. Timpanaro, N. Moltabetti, I. L. Reisin, M. A. Arnaout, and H. F. Cantiello.** 2002. Voltage dependence and pH regulation of human polycystin-2 mediated cation channel activity. J. Biol. Chem. **277:**24959–24966.
11. **Guo, L., T. H. Schreiber, S. Weremowicz, C. C. Morton, C. Lee, and J. Zhou.** 2000. Identification and characterization of a novel polycystin family member, polycystin-L2, in mouse and human: sequence, expression, alternative splicing, and chromosomal localization. Genomics **64:**241–251.
12. **Hamill, O. P., A. Marty, E. Neher, B. Sakmann, and F. J. Sigworth.** 1981. Improved patch-clamp techniques for high-resolution current recording from cells and cell-free membrane patches. Pflugers Arch. **391:**85–100.
13. **Hanaoka, K., F. Qian, A. Boletta, A. K. Bhunia, K. Piontek, L. Tsiokas, V. P. Sukhatme, W. B. Guggino, and G. G. Germino.** 2000. Co-assembly of polycystin-1 and -2 produces unique cation-permeable currents. Nature **408:**990–994.
14. **Hou, X., M. Mrug, B. K. Yoder, E. J. Lefkowitz, G. Kremmidiotis, P. D'Eustachio, D. R. Beier, and L. M. Guay-Woodford.** 2002. Cystin, a novel cilia-associated protein, is disrupted in the cpk mouse model of polycystic kidney disease. J. Clin. Investig. **109:**533–540.
15. **Hughes, J., C. J. Ward, R. Aspinwall, R. Butler, and P. C. Harris.** 1999. Identification of a human homologue of the sea urchin receptor for egg jelly: a polycystic kidney disease-like protein. Hum. Mol. Genet. **8:**543–549.
16. **Hughes, J., C. J. Ward, B. Peral, R. Aspinwall, K. Clark, J. L. San Millan, V. Gamble, and P. C. Harris.** 1995. The polycystic kidney disease 1 (PKD1) gene encodes a novel protein with multiple cell recognition domains. Nat. Genet. **10:**151–160.
17. **Ibraghimov-Beskrovnaya, O., W. R. Dackowski, L. Foggensteiner, N. Coleman, S. Thiru, L. R. Petry, T. C. Burn, T. D. Connors, T. Van Raay, J. Bradley, F. Qian, L. F. Onuchic, T. J. Watnick, K. Piontek, R. M. Hakim, G. M. Landes, G. G. Germino, R. Sandford, and K. W. Klinger.** 1997. Polycystin: in vitro synthesis, in vivo tissue expression, and subcellular localization identifies a large membrane-associated protein. Proc. Natl. Acad. Sci. USA **94:**6397–6402.
18. **Jensen, T. J., M. A. Loo, S. Pind, D. B. Williams, A. L. Goldberg, and J. R. Riordan.** 1995. Multiple proteolytic systems, including the proteasome, contribute to CFTR processing. Cell **83:**129–135.
19. **Koulen, P., Y. Cai, L. Geng, Y. Maeda, S. Nishimura, R. Witzgall, B. E. Ehrlich, and S. Somlo.** 2002. Polycystin-2 is an intracellular calcium release channel. Nat. Cell Biol. **4:**191–197.
20. **Mochizuki, T., G. Wu, T. Hayashi, S. L. Xenophontos, B. Veldhuisen, J. J. Saris, D. M. Reynolds, Y. Cai, P. A. Gabow, A. Pierides, W. J. Kimberling, M. H. Breuning, C. C. Deltas, D. J. Peters, and S. Somlo.** 1996. PKD2, a gene for polycystic kidney disease that encodes an integral membrane protein. Science **272:**1339–1342.
21. **Nauli, S. M., F. J. Alenghat, Y. Luo, E. Williams, P. Vassilev, X. Li, A. E. H. Elia, W. Lu, E. M. Brown, S. J. Quinn, D. E. Ingber, and J. Zhou.** 2003. Polycystins 1 and 2 mediate mechanosensation in the primary cilium of kidney cells. Nat. Genet. **33:**129–137.
22. **Newby, L. J., A. J. Streets, Y. Zhao, P. C. Harris, C. J. Ward, and A. C. Ong.** 2002. Identification, characterization, and localization of a novel kidney polycystin-1-polycystin-2 complex. J. Biol. Chem. **277:**20763–20773.
23. **Nomura, H., A. E. Turco, Y. Pei, L. Kalaydjieva, T. Schiavello, S. Weremowicz, W. Ji, C. C. Morton, M. Meisler, S. T. Reeders, and J. Zhou.** 1998. Identification of PKDL, a novel polycystic kidney disease 2-like gene whose murine homologue is deleted in mice with kidney and retinal defects. J. Biol. Chem. **273:**25967–25973.
24. **Parnell, S. C., B. S. Magenheimer, R. L. Maser, C. A. Zien, A. M. Frischauf, and J. P. Calvet.** 2002. Polycystin-1 activation of c-Jun N-terminal kinase and AP-1 is mediated by heterotrimeric G proteins. J. Biol. Chem. **277:**19566–19572.
25. **Pazour, G. J., S. A. Baker, J. A. Deane, D. G. Cole, B. L. Dickert, J. L. Rosenbaum, G. B. Witman, and J. C. Besharse.** 2002. The intraflagellar transport protein, IFT88, is essential for vertebrate photoreceptor assembly and maintenance. J. Cell Biol. **157:**103–113.
26. **Pazour, G. J., J. T. San Agustin, J. A. Follit, J. L. Rosenbaum, and G. B. Witman.** 2002. Polycystin-2 localizes to kidney cilia and the ciliary level is elevated in orpk mice with polycystic kidney disease. Curr. Biol. **12:**R378–R380.
27. **Peters, D. J., A. van de Wal, L. Spruit, J. J. Saris, M. H. Breuning, J. A. Bruijn, and E. de Heer.** 1999. Cellular localization and tissue distribution of polycystin-1. J. Pathol. **188:**439–446.
28. **Qian, F., F. J. Germino, Y. Cai, X. Zhang, S. Somlo, and G. G. Germino.** 1997. PKD1 interacts with PKD2 through a probable coiled-coil domain. Nat. Genet. **16:**179–183.
29. **Sato, S., C. L. Ward, M. E. Krouse, J. J. Wine, and R. R. Kopito.** 1996.

Glycerol reverses the misfolding phenotype of the most common cystic fibrosis mutation. J. Biol. Chem. **271:**635–638.
30. **Scheffers, M. S., H. Le, P. van der Bent, W. Leonhard, F. Prins, L. Spruit, M. H. Breuning, E. de Heer, and D. J. Peters.** 2002. Distinct subcellular expression of endogenous polycystin-2 in the plasma membrane and Golgi apparatus of MDCK cells. Hum. Mol. Genet. **11:**59–67.
31. **Taulman, P. D., C. J. Haycraft, D. F. Balkovetz, and B. K. Yoder.** 2001. Polaris, a protein involved in left-right axis patterning, localizes to basal bodies and cilia. Mol. Biol. Cell **12:**589–599.
32. **Tsien, R., and T. Pozzan.** 1989. Measurement of cytosolic free Ca^{2+} with quin2. Methods Enzymol. **172:**230–262.
33. **Tsiokas, L., T. Arnould, C. Zhu, E. Kim, G. Walz, and V. P. Sukhatme.** 1999. Specific association of the gene product of *PKD2* with the TRPC1 channel. Proc. Natl. Acad. Sci. USA **96:**3934–3939.
34. **Tsiokas, L., E. Kim, T. Arnould, V. P. Sukhatme, and G. Walz.** 1997. Homo- and heterodimeric interactions between the gene products of PKD1 and PKD2. Proc. Natl. Acad. Sci. USA **94:**6965–6970.
35. **Valentijn, J. A., G. K. Fyfe, and C. M. Canessa.** 1998. Biosynthesis and processing of epithelial sodium channels in *Xenopus* oocytes. J. Biol. Chem. **273:**30344–30351.
36. **Vassilev, P. M., L. Guo, X. Z. Chen, Y. Segal, J. B. Peng, N. Basora, H. Babakhanlou, G. Cruger, M. Kanazirska, C. Ye, E. M. Brown, M. A. Hediger, and J. Zhou.** 2001. Polycystin-2 is a novel cation channel implicated in defective intracellular Ca^{2+} homeostasis in polycystic kidney disease. Biochem. Biophys. Res. Commun. **282:**341–350.
37. **Ward, C. L., S. Omura, and R. R. Kopito.** 1995. Degradation of CFTR by the ubiquitin-proteasome pathway. Cell **83:**121–127.
38. **Wu, G., T. Hayashi, J. H. Park, M. Dixit, D. M. Reynolds, L. Li, Y. Maeda, Y. Cai, M. Coca-Prados, and S. Somlo.** 1998. Identification of PKD2L, a human PKD2-related gene: tissue-specific expression and mapping to chromosome 10q25. Genomics **54:**564–568.
39. **Yoder, B. K., A. Tousson, L. Millican, J. H. Wu, C. E. Bugg, Jr., J. A. Schafer, and D. F. Balkovetz.** 2002. Polaris, a protein disrupted in orpk mutant mice, is required for assembly of renal cilium. Am. J. Physiol. Renal Physiol. **282:**F541–F552.
40. **Yuasa, T., B. Venugopal, S. Weremowicz, C. C. Morton, L. Guo, and J. Zhou.** 2002. The sequence, expression, and chromosomal localization of a novel polycystic kidney disease 1-like gene, PKD1L1, in human. Genomics **79:**376–386.